Drone remote sensing over a late Iron Age/ Roman period landscape in Lionserpolder, Friesland

Jitte Waagen, Rik Feiken

University of Amsterdam

4D Research Lab

The 4D Research Lab Report Series has been established as an instrument to promote transparency regarding the 4DRL virtual visualisation projects, workflow and pipeline development and technical experiments. The aim is to maximize knowledge sharing, meta- and paradata communication and clarification of author- and ownership of 4D Research Lab products.

Jitte Waagen, Tijm Lanjouw

Drone remote sensing over a late Iron Age/Roman period landscape in Lionserpolder, Friesland

4D Research Lab Report Series 5

Author(s): Jitte waagen, Rik Feiken
Layout: Mikko Kriek
Editor(s): Jitte Waagen, Tijm Lanjouw

ISSN 2772-7734

January 2024

http://4dresearchlab.nl

1 Project datasheet

Name project	Drone remote sensing over a late Iron Age/Roman period landscape in the Lionserpolder, Friesland
Date (from – to)	07/10/2021
Author(s) of report	Jitte Waagen, 4D Research Lab Rik Feiken, Rijksdienst voor het Cultureel Erfgoed
Project initiators	Menno van der Heiden, Rik Feiken, Rijksdienst voor het Cultureel Erfgoed
Execution	Jitte Waagen, 4D Research Lab: project management, fieldwork, research, data modeling, reporting Mikko Kriek, 4D Research Lab: fieldwork
Scientific advice	NA
Delivered product(s)	Projected sensor data, raster files, generated maps/visualisations
Where to access main outcomes/product	Available on request at the 4D Research Lab. Contact Jitte Waagen (j.waagen@uva.nl).
Location and accessibility of project files	4D Research Lab archive, cloud storage. Available on request at the 4D Research Lab. Contact Jitte Waagen (j.waagen@uva.nl).
Related publications	NA

2 Aims and justification

2.1 *Abstract*

The drone remote sensing operations were commissioned by the Rijksdienst voor het Cultureel Erfgoed (RCE), by archaeologist drs. Menno van der Heiden. The project research and reporting on the RCE side has subsequently been taken over by archaeologist dr. Rik Feiken. The area under investigation is an Iron Age/Roman period landscape surrounding an unexcavated site, probably a late Iron Age/Roman period (LIA/R) farm. There are clear patterns of LIA/R habitation, observed through ditches that are likely of LIA/R origin, and LIA/R pottery retrieved from test corings and test trenches. The expected habitation is situated on an 'island', known as 'Het Eiland', an isolated stretch of land in a former salt marsh landscape, that is not visible as a habitation mound. More common in this area are so-called 'terpen' which are clearly visible as anthropogenic elevated areas, so this is a relatively rare phenomenon (Feiken & van der Heiden, 2018). The surrounding landscape may still be a largely intact late Iron Age landscape with old watercourses and salt marshes ('kwelders') still visible in the terrain morphology, and possible offsite archaeological remains. Therefore, a drone remote sensing operation was considered to be an effective method to map potentially present remains of the local LIA/R past.

2.2 *Introduction*

2.2.1 *Overview: site and research questions*

The site 'Het Eiland' is situated around 650m to the southwest of the hamlet Hesens in Friesland (fig. 1). It has been researched using aerial photographs, the AHN3 (https://www.pdok.nl/downloads/-/article/actueel-hoogtebestand-nederland-ahn3) and test corings (14 in total). The site appears to be a silted Late Iron Age/ Roman period farm that has been preserved well. As the landscape from that period appears to have been preserved to a large degree as well, a broader research area has been defined. The specific aim of the drone remote sensing operations, therefore, is to map the paleo landscape surrounding 'Het Eiland', including potential offsite archaeology such as ditches and paths. The eventual aim is to answer the question if the site and landscape around it can be nominated as an Archaeological Monument. In October 2021, a drone remote sensing operation was executed, making use of optical and multispectral sensors. Their basic workings are described here, with their potential output for archaeological prospection (for methodological discussion, see e.g., Waagen 2023).

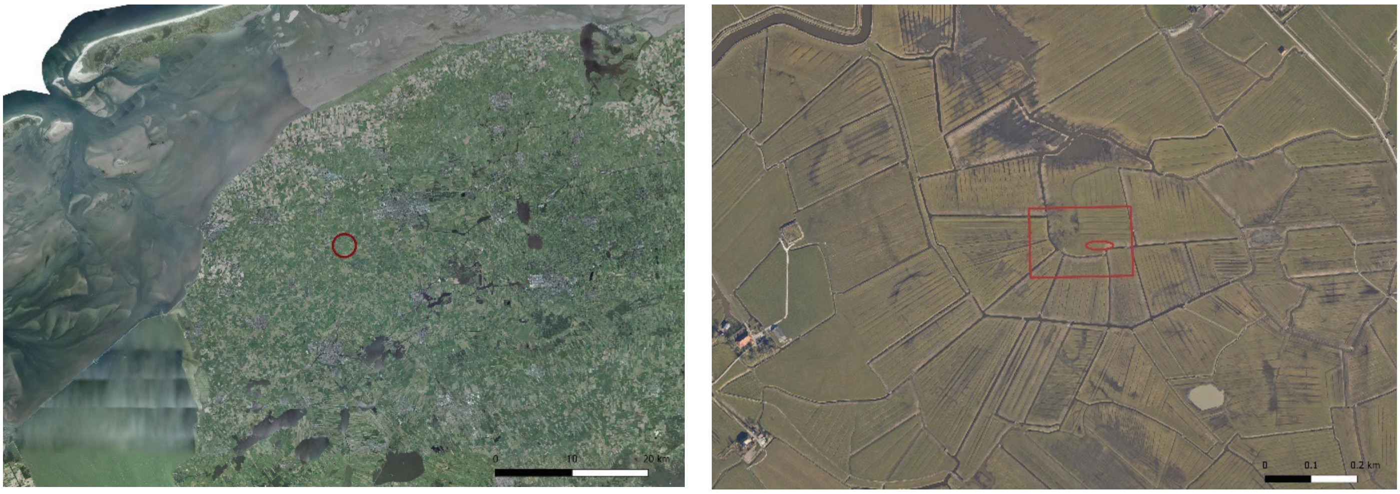

Figure 1. Research area, left: location of Lionserpolder in Friesland, right: main research area and indication of habitation site 'Het Eiland'.

2.2.2 Optical

Optical sensors, i.e., visible-light cameras, can be deployed using UAS platforms to collect high-resolution aerial photographs. Using photogrammetric techniques through a combination of computer vision techniques and geometrical triangulation, individual photos can be relatively positioned, and their pixel data combined to project 3D points, create a 3D mesh and project photorealistic textures on that mesh. The mesh as well as 3D point clouds can be used to create, among other products, both mosaicked aerial orthophotos as well as digital elevation models, that can help identify cropmarks and soil marks, as well as earthworks. Furthermore, they are very valuable for comparison with other sensor data to understand whether identified anomalies are likely archaeological features, or may be explained by other human-, topographical or landscape features.

2.2.3 Multispectral

Multispectral sensors record visible light as well as part of the invisible electromagnetic spectrum in separate bands on different sensors, resulting in different reflectance images, typically Blue (centre wavelength: 475 nm), Green (centre wavelength: 560 nm), Red (centre wavelength: 668 nm), Rededge (centre wavelength: 772 nm), and Near-Infrared (centre wavelength: 840 nm), although different combinations and (slightly diverging) wavelengths are possible. Since the degree to which different materials absorb or reflect radiation of different wavelengths varies, the exact reflectance values can provide information about their physical compositions. This can make observations possible beyond human eyesight; for example, cropmarks can be greatly enhanced because more healthy vegetation reflects relatively more Near-Infrared radiation but absorbs more visible light. Using photogrammetric techniques similar as with optical data, mosaicked reflectance maps can be created. The various wavelength reflectance maps can be part of many equations that emphasize various aspects of vegetation, for example Normalized Difference Vegetation Index (NDVI) often used for agricultural purposes.

3 Historical context

Traces of an old settlement occur on ‘Het Eiland’, which is then further covered by a zone where no buried archaeological remains are expected (off site area). The settlement on ‘Het Eiland’ probably consists of a terp mound, almost invisible in the field due to later marine sedimentation. In the direct surroundings of the terp ditches occur of which two were examined using small trial trenches in 2021 (Feiken & Van der Heiden 2023). There is no direct evidence for prehistoric infrastructural works (such as paths and dikes) or agricultural fields, but it is likely they do occur just outside the terp. (Ritual) deposits and burials may also be present here.

The oldest collected pottery material ('terpaardewerk') on ‘Het Eiland’ dates from the middle Iron Age. Based on the archaeological finds, the site can be dated from the (late) Iron Age to (early) Roman period. The ditches also originate from this period. Fields, dikes, paths, burials and (ritual) depots, found at other excavated terp mounds, also commonly date from the (late) Iron Age to the (early) Roman period.
After the 2016 coring campaign the size of the terp was estimated at about 40 by 15 m. The system of ditches itself extends over a large area, on and around ‘Het Eiland’. The possible ditches on ‘Het Eiland’ itself are several tens of meters in length and are about 3-4 meters wide. Based on the coring campaign, nothing can yet be said about the extent of possible fields, dikes, paths, burials and (ritual) depots.

Terp mounds are characterized in excavations by clearly recognizable dark coloured layers containing material such as pottery, charcoal, and bone. There are soil marks in the form of post marks, pits, ditches, trenches, and sod tracks. The ditches are easily recognized as soils marks during an excavation, and recognizable on the AHN as relatively lower situated, linear features. Ditches contain a lot of archaeological material on ‘Het Eiland’. Fields will be recognizable by old, tilled layers and plough/spit tracks. Dikes will be recognizable during excavations as stacking of sods. Paths will be recognizable as an eroded tread. Burials consist of human remains with secondary gifts or cremation remains in an urn. (Ritual) depots probably consist of (burned or unburned) human and animal bone material combined with pottery or metal objects.

4 Documentation and research design

4.1 Documentation and modelling workflows

This section elaborates on the data acquisition procedure per sensor, documentation workflow adapted from Lozić and Štular (2021) with modifications for different sensor types.

4.1.1 Raw data acquisition and processing

The area has been visited in October 2021 (fig. 2).

The flight operations in October were not optimal; the ground was very wet due to rain the days before, scattered clouds (causing variable light conditions) and cool climate grass in full growth. Flight moments were set for optimal results, i.e., optical at noon (solar angle at maximum zenith), multispectral within 2 hours of the solar noon and thermal after sunset. The flight altitudes were set to result in an optimal GSD, around 1 cm/pixel for the optical recordings, and around 3 cm/pixel for the multispectral recording.

See appendix 1 for the documented data capture parameters.

Figure 2. Research area, photo taken in October 2021 from the southwest towards the northeast.

4.1.2 *Data Processing and Derivation of the Products*

Data processing is described here per type of data briefly, as the procedures are similar for different datatypes.

Optical sensor data

For the optical datasets, processing is rather straightforward. Geotagged images are, after a quick manual inspection on quality, imported into photogrammetric software, in this case Pix4D. They are integrated with the differential GPS data in the form of geolocated targets that are visible on the images. Images are run through a process of internal and external alignment (called calibration in Pix4D), dense point cloud and 3D mesh generation and finally processed into digital elevation models and orthophotos (for technical explanations, see e.g., Sapirstein and Murray 2017). Final visualisation is done by generating a multiband colour (RGB) raster that can be directly imported and inspected in GIS (QGIS).

Multispectral sensor data

For the multispectral datasets, processing is a bit more involving. Five different images are generated in every single capture moment (using [..]_1.tif, [..]_2.tif etc. suffixes): images that store reflectance values in respectively the Red (R), Green (G), Blue (B), Rededge (RE) and Near Infrared (NIR) band. Again, geotagged images are, after a quick manual inspection on quality, imported into photogrammetric software, in this case Pix4D. Here, they are calibrated using the photos made in the field of the reflectance target as well as the data in the EXIF of the Downwelling Light Sensor. This compensates for any major changes in the radiation from the sun during the recording and between recordings. Then, using the set of images with the reflectance in the Green band, the process follows the common photogrammetric procedure; images are integrated with the differential GPS data in the form of geolocated targets that are visible on the images; images are run through a process of internal and external alignment (called calibration in Pix4D), and a dense point cloud is generated.

Based on the generated point cloud index maps can be generated. The captured reflectance in the different bands is projected onto the individual pixels of a generated orthophoto, which are the RGB, RE and NIR bands. The different reflectance values can also be used to generate different kinds of indices, usually called Vegetation Indices (VIs). The software allows to make such calculations and generate new index maps. A very common example is the Normalized Difference Vegetation Index (NDVI) indicating relative plant health, calculated by:

$$NDVI = \frac{(\mathrm{NIR} - \mathrm{R})}{(\mathrm{NIR} + \mathrm{R})}$$

Eventual visualisation is done by importing and inspecting the different indices in GIS (QGIS). Raster values can be visualised using the singleband pseudocolour option. For this project, the interactive local cumulative cut stretch toolset of QGIS has been used to generate different enhanced visualisations.

See appendix 2 for the documented data processing parameters.

4.1.3 (Archaeological) interpretation

The archaeological interpretation is a stepped process. First of all, visualisation leads to first identification of potential anomalies, and comparative analysis provides clues as to their origins. Anomalies are mostly identified through relative contrasts in sensor readings. Although the sensors do provide accurate elevation points, temperatures, reflectance values, etc., such absolute values are largely not directly relevant for archaeological prospection purposes. The interpretation process starts with an integrative approach in which all contextual data is retrieved (e.g., from online data portals) and added to the dataset. Anomalies will be compared with all other data layers in order to be able to isolate the potential archaeological evidence. In a subsequent step, identified anomalies, i.e., a data model based on relative sensor readings of features that cannot be clearly explained by natural or modern anthropomorphic activity, will be evaluated in terms of potential archaeological interpretation. This process is mostly guided through contextual and typological analyses, and eventually results in an archaeological model. It must be mentioned that this often plays out as an iterative process between primary data processing, enhanced visualisation, and mapping interpretation.

Contextual data

Contextual data for this project was available as satellite imagery from both Google Earth and the satellietdataportaal.nl. Also, various data layers available through Publieke Dienstverlening op de Kaart (PDOK plugin in QGIS) have been inspected, i.e., 25cm aerial photographs and thermal infrared coverage. Also, the AHN4 has been downloaded and inspected (https://www.pdok.nl/introductie/-/article/actueel-hoogtebestand-nederland-ahn). Since the study of these datasets have already been reported on in a preceding inventory (Feiken & van der Heiden, 2023), they will not be elaborately dealt with here (fig. 3).

Mapping and interpretation

Following the workflows described above, a total of 15 anomalies have been identified. They are discussed in detail in this section. Anomalies have all been mapped on the various visualisations of the DEM data model derived from the optical survey (fig. 5-10), but the optical orthophoto (fig. 4) and NDVI data model derived from the multispectral survey are also included (fig. 11).

See appendix 3 for a description of the documented metadata in the table.

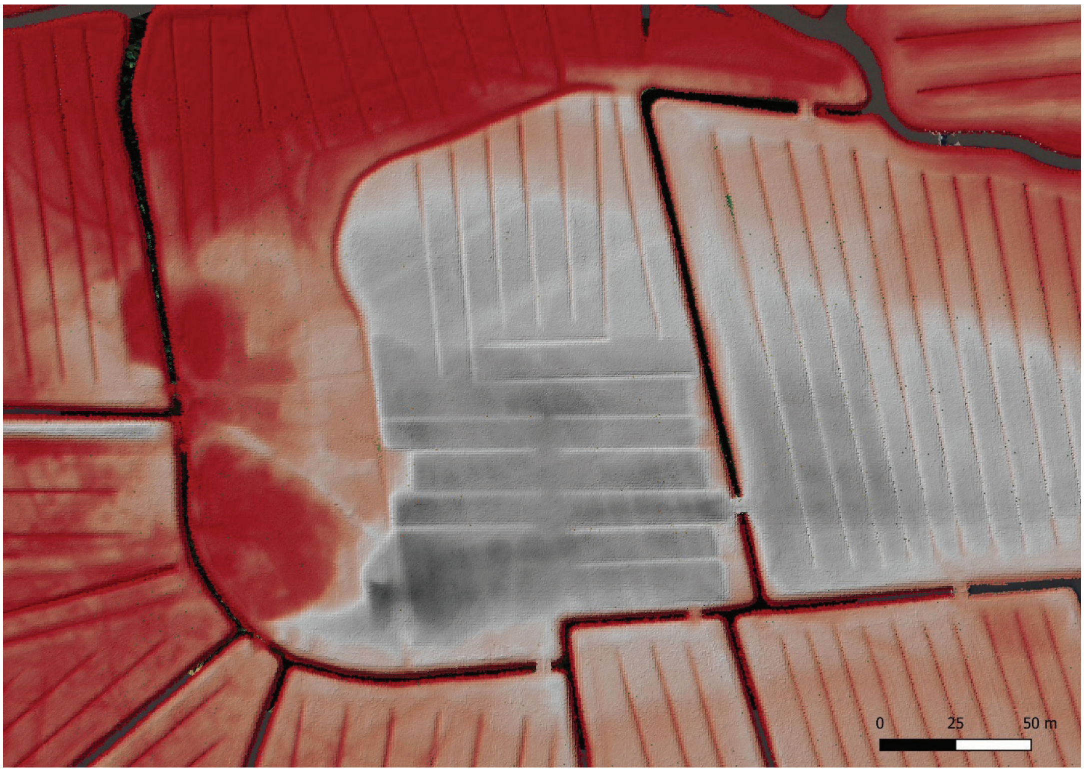

Figure 3. AHN3 visualisation using hillshade.

Figure 4. Drone orthophoto (optical sensor) with habitation site indication (white circle)

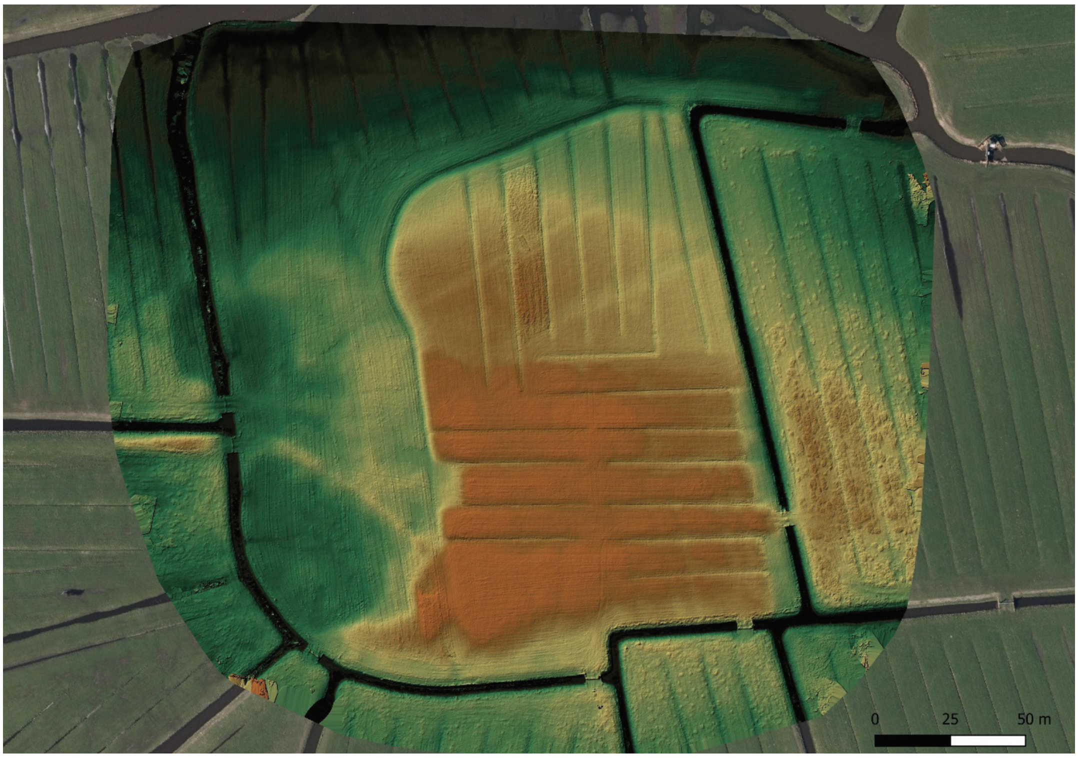

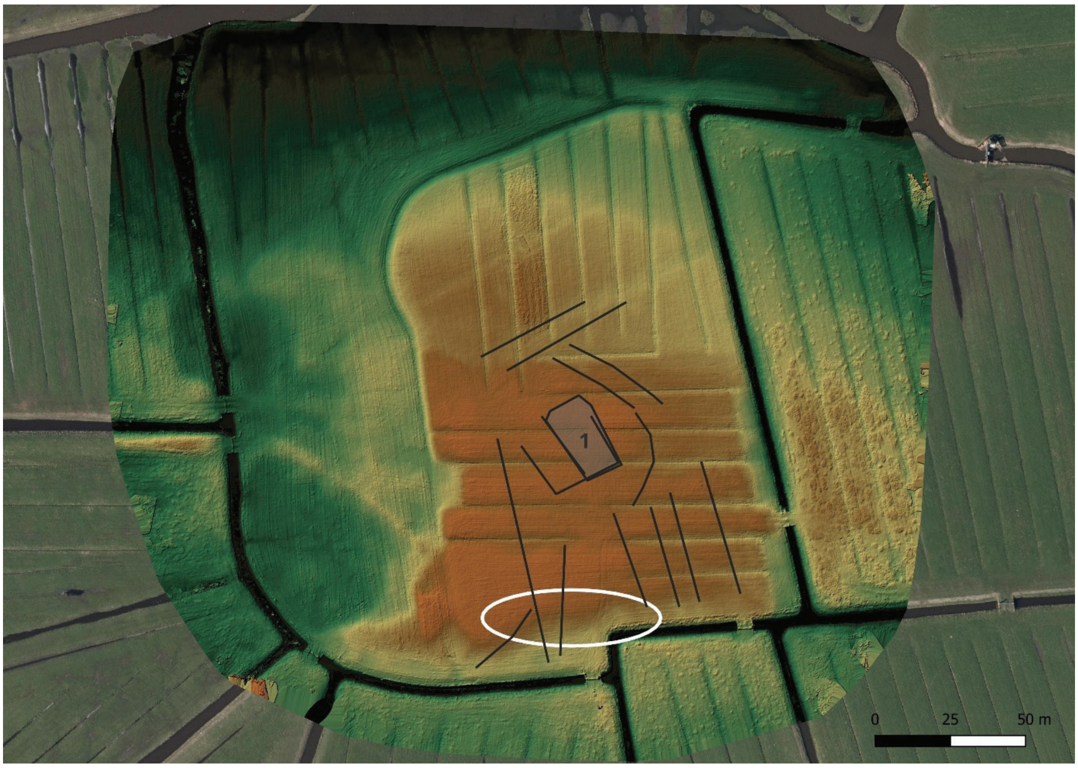

Figure 5-6. Drone DEM with hillshade version 1 (optical sensor) with habitation site indication (white circle) obtained by test corings (Feiken & van der Heiden 2018), and with indicated anomalies (anomalies 2-15 are indicated by the unnumbered black lines).

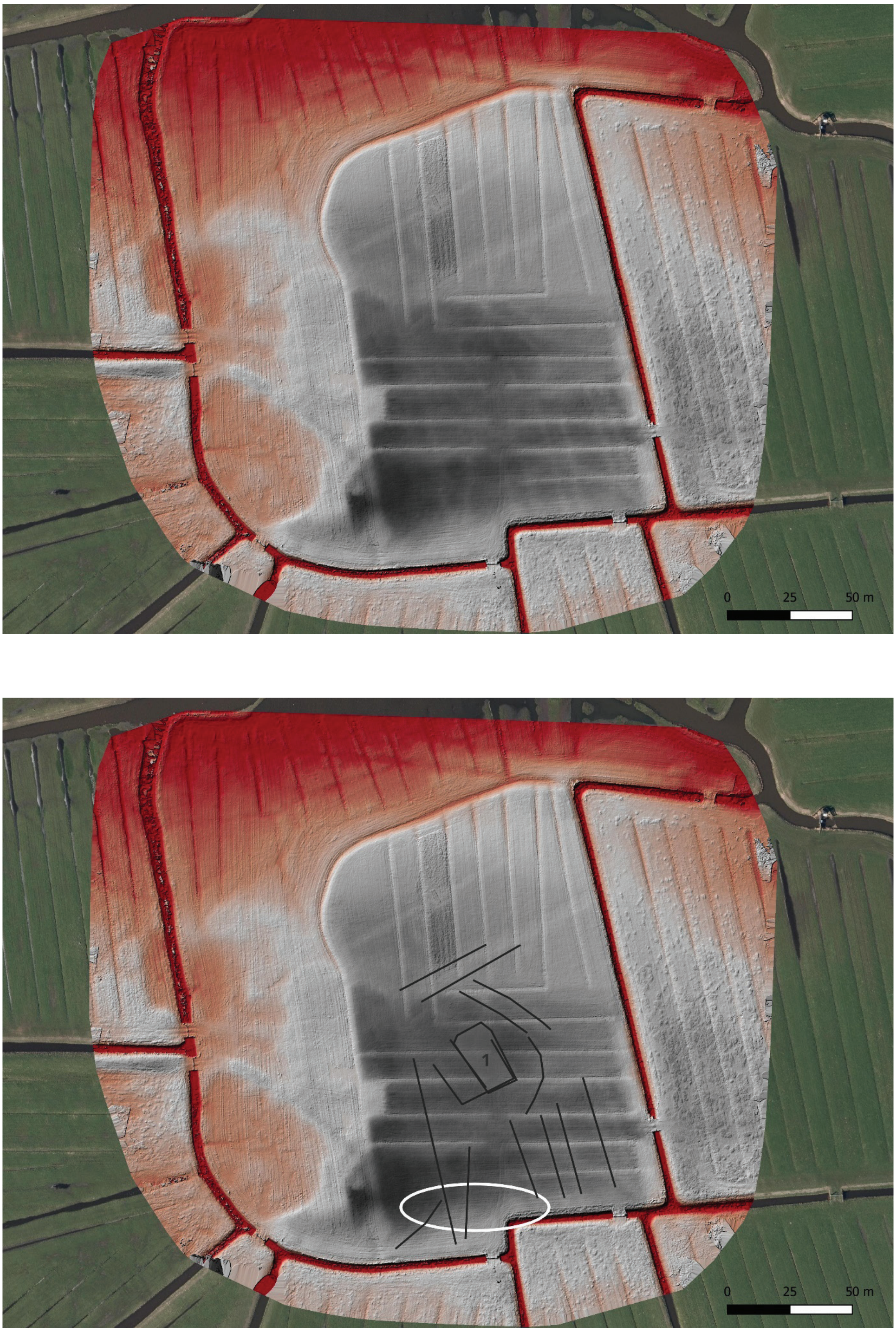

Figure 7-8. Drone DEM with hillshade version 2 (optical sensor) with habitation site indication (white circle) obtained by test corings (Feiken & van der Heiden 2018), and with indicated anomalies (anomalies 2-15 are indicated by the unnumbered black lines).

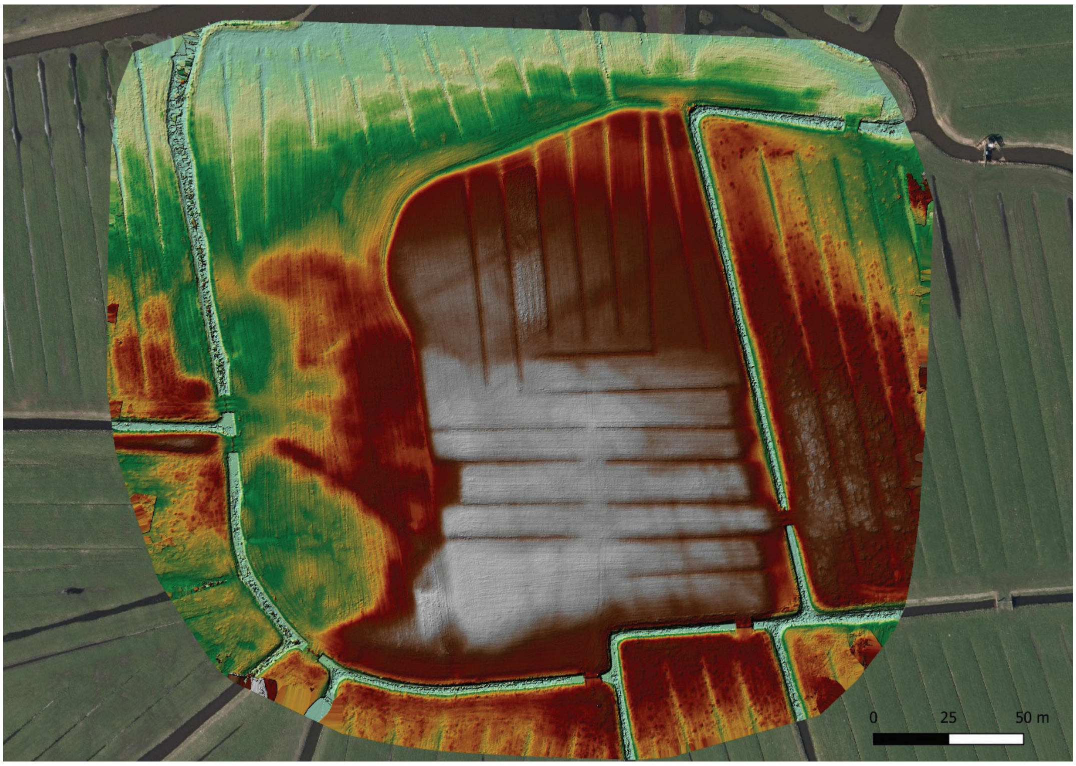

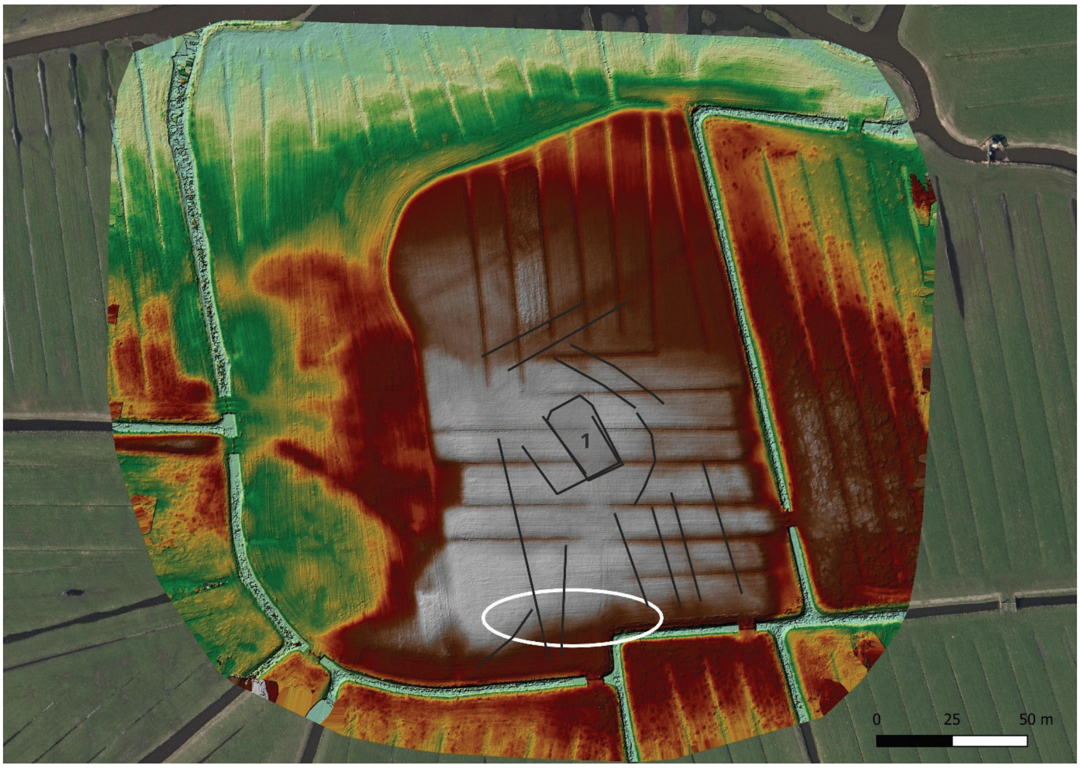

Figure 9-10. Drone DEM with hillshade version 3 (optical sensor) with habitation site indication (white circle) obtained by test corings (Feiken & van der Heiden 2018), and with indicated anomalies (anomalies 2-15 are indicated by the unnumbered black lines).

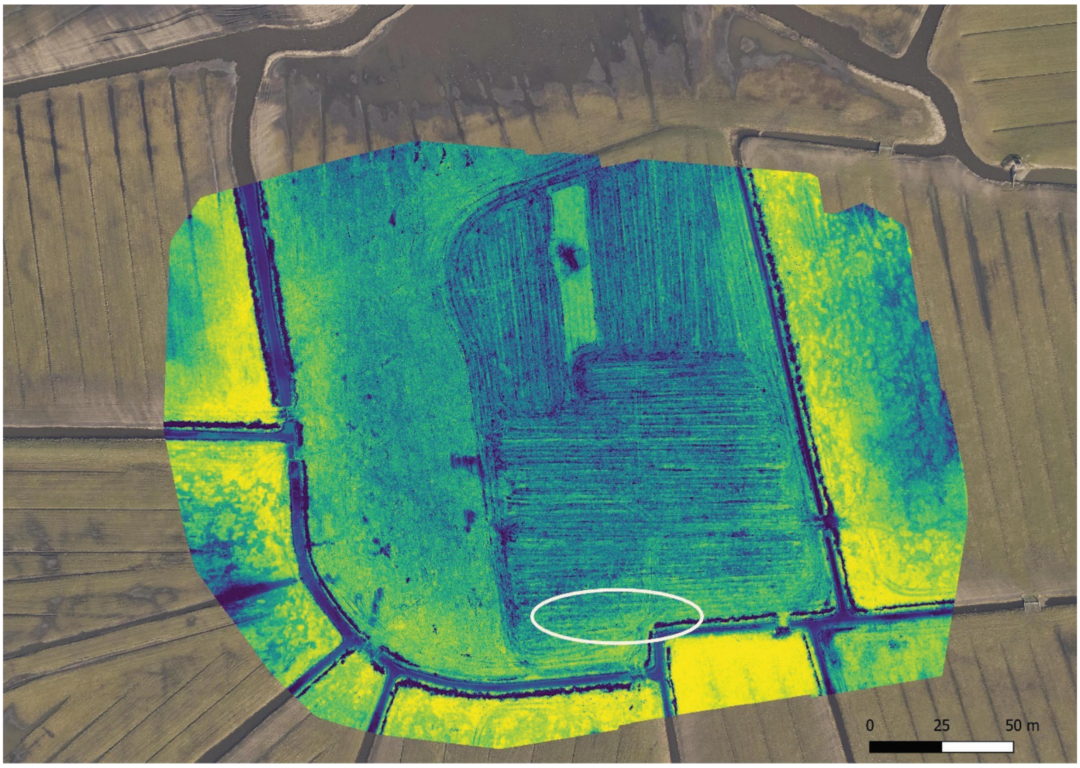

Figure 11. Drone NDVI (multispectral sensor) with habitation site indication (white circle)

All mapping (fig. 5-10) by RF/JW, 20-11-2023 (all vegetation densities: 2)

id	source_lay	anoma_int	an_confid	visibility	arch_int	arch_conf
1	Lions_optical_45m_12	rectangular feature, delineated by depressions	2	2	unclear, but delineated by ditches	2
2	Lions_optical_45m_12	elongated narrow depression	3	2	ditch, drainage	3
3	Lions_optical_45m_12	elongated narrow depression	3	2	ditch, drainage	3
4	Lions_optical_45m_12	elongated narrow depression	3	2	ditch, drainage	3
5	Lions_optical_45m_12	elongated narrow depression	3	2	ditch, drainage	3
6	Lions_optical_45m_12	elongated narrow depression	3	2	ditch, drainage	3
7	Lions_optical_45m_12	elongated narrow depression	3	2	ditch, drainage	3
8	Lions_optical_45m_12	elongated narrow depression	3	2	ditch, drainage	3
9	Lions_optical_45m_12	elongated narrow depression	3	2	ditch, drainage	3
10	Lions_optical_45m_12	elongated narrow depression	3	2	ditch, drainage	3
11	Lions_optical_45m_12	elongated narrow depression	3	2	ditch, drainage	3
12	Lions_optical_45m_12	elongated narrow depression	3	2	ditch, drainage	3
13	Lions_optical_45m_12	elongated narrow depression	3	2	ditch, drainage	3
14	Lions_optical_45m_12	elongated narrow depression	3	2	ditch, drainage	3
15	Lions_optical_45m_12	elongated narrow depression	3	2	ditch, drainage	3

Remarks

The DEM visualisations show various earthworks that can be archeologically interpreted. The most conspicuous anomalies are the various linear structures, represented by shallow elevation depressions that run predominantly roughly north-south, that are interpreted as possible LIA/R ditches/drainage waterways. It appears these may be connected to the attested habitation on 'Het Eiland', indicated by the white circle. In addition, anomaly 1 appears to be a rectangular structure measuring 26 x 14 m. Its interpretation is currently unclear but could be related to a habitation structure.

4.1.4 Deep interpretation

Based on the drone remote sensing results, a series of very fine maps of the current vegetation status and morphology of the terrain has been produced. The terrain morphology as visible on the various DEM with hillshade enhancement versions is clearly pronounced, with the island ('Het Eiland') dominant as a slight elevation in the center, and various indications of LIA/R landscape features such as those already visible on the AHN, i.e., old watercourses, as well as cultural features such as ditches, as well as those clearly identifiable on the various DEM visualisations, which are interpreted as ditches/drainage waterways and a potential habitational structure. The orthophoto and the multispectral vegetation index mosaics are showing vegetation without any clear indications of past land use or other activity.

In the autumn of 2023, there will be a physical assessment of the identified anomalies on 'Het Eiland' by trial trenches and an extended coring campaign.

4.1.5 Conclusion

The drone remote sensing operations have produced clear visualisations of Iron Age/Roman period natural and cultural landscape features. However, no indications of buried archaeological deposits have been traced through the remote sensing campaign.

5 Dissemination and archiving

5.1 Data management

All data is stored at the 4D Research Lab archive, cloud storage (MS Teams/ Sharepoint), facility of the UvA. In the near future, the original data will be published on the UvA Figshare environment. Original raw material is saved alongside all derived products. These consist of calibrated images (.jpg, .tif), field measurements (.txt), photogrammetry project files and related data (.p4d, .qgz), and raster products such as orthophotos, DEMs/DTMs, Vis, etc. (geotiff, .tif). The total project size is ca. 53 GB. The 4DRL uses a standardized GIS folder structure, but still has to implement a metadata schema for individual files.

5.2 Dissemination

This report will be published open access through the 4D Research Lab Report Series, a Figshare hosted Journal, and be provided with a DOI. As such, existing metadata will be preserved, and the data will be rendered as FAIR as possible.

5.3 Archiving

As for archiving, as mentioned, all raw data will eventually be made available via Figshare. In addition, the project data will remain available at the cloud storage facility of the UvA (MS Teams/Sharepoint). All data will be kept available for use/re-use upon any reasonable request.

6 Bibliography

- Feiken, H. and van der Heiden, M. 2018. Onderzoek met uitzicht. Karterend booronderzoek in de Lionserpolder, gemeente Leeuwarden. Rijksdienst voor het Cultureel Erfgoed, Rapportage Archeologische Monumentenzorg, 246.

- Feiken, H. and van der Heiden, M. 2023. Een cultuurlandschap uit de ijzertijd-Romeinse tijd in de Lionserpolder (gemeente Leeuwarden). Oppervlaktekarteringen en booronderzoek 2020. Rijksdienst voor het Cultureel Erfgoed, Rapportage Archeologische Monumentenzorg, 275.

- Lozić, E., Štular, B., 2021. Documentation of Archaeology-Specific Workflow for Airborne LiDAR Data Processing. *Geosciences* 11, no. 1: 26. https://doi.org/10.3390/geosciences11010026

- Sapirstein, P., Murray, S., 2017. Establishing best practices for photogrammetric recording during archaeological fieldwork. J. Field Archaeol. 42 (4), 337–350. https://doi.org/10.1080/00934690.2017.1338513

- Waagen, J. (2023). 4DRL Report Series 4 - In search of a castle: Multisensor UAS research at the Medieval site of 't Huijs ten Bosch, Weesp. University of Amsterdam / Amsterdam University of Applied Sciences. Journal contribution. https://doi.org/10.21942/uva.23375486.v3

Appendix 1, data capture parameters

Project planning	Title	Drone remote sensing over an Iron Age landscape in Lionserpolder, Friesland
	Brief description	Iron Age landscape mapping
	Purpose	Map eventual Iron Age landscape and past features related to habitation
	Platform	Multirotor
	Date of flight(s)	7-10-2021
	Operator	UvA Dronelab (4DRL)
	Pilot in Command	Jitte Waagen
	Observers	Mikko Kriek

Optical survey

System calibration	Sensor type	Optical, CMOS, 4/3”
	Scanner/camera model	Zenmuse X5S
	Lens	15mm
	Shutter type	Rolling (fast readout)
	Instruments	DJI M210, Geomax Zenith15 dGPS
	Pixels	20.8MP
	Precision	5280x3956
	Accuracy	N/A
Data acquisition	Time	12.30
	Exposure triangle	Aperture Priority (f/2.8)
	Altitude Above Ground Level	45m
	Average Speed	3.5m/s
	Overlap (side- and front)	70% and 80%
	Estimated type archaeology	Ditches, natural Iron Age landscape features
	Estimated depth archaeology	30-100cm
	Vegetation type	Grassland
	Vegetation state	Full growth (fall period of cool climate grass)
	Moisture conditions	Dry, soil quite wet
	Superficial layer	Light clay
	Soil matrix	Light clay
	Light conditions	Scattered clouds
	Number of photos	399

	Format	JPG
Geometric correction	Flight trajectory calculation (software/method)	DJI Pilot/grid
	GCPs used	8
	GCP geolocation instrument	Geomax Zenith15, 06GPS
	GCP geolocation accuracy	1-2cm
	GCP and photo merging	Pix4D
	Coordinate system	Amersfoort/RD New (EGM 96 Geoid), EPSG: 28992
Radiometric correction	N/A	N/A

Multispectral survey

System calibration	Sensor type	Multispectral, 4/3”
	Scanner/camera model	Micasense Rededge
	Centre bandwidths	B (475), G (560), R (668), RE (717), NIR (840)
	Lens	5.4mm
	Shutter type	Global (all sensors)
	Instruments	DJI M210, Geomax Zenith15 dGPS, Downwelling Light Sensor 2
	Pixels	1.2MP (all sensors)
	Precision	1280x960 (all sensors)
	Accuracy	N/A
Data acquisition	Time	13.00
	Exposure triangle	Automated
	Altitude Above Ground Level	45m
	Average Speed	3m/s
	Overlap (side- and front)	70% and 80%
	Estimated type archaeology	Ditches, natural Iron Age landscape features
	Estimated depth archaeology	30-100cm
	Vegetation type	Grassland
	Vegetation state	Full growth (fall period of cool climate grass)
	Moisture conditions	Dry, soil quite wet
	Superficial layer	Light clay
	Soil matrix	Light clay
	Light conditions	Scattered clouds
	Number of photos	2690
	Format	TIF

Geometric correction	Flight trajectory calculation (software/method)	DJI Pilot/grid
	GCPs used	8
	GCP geolocation instrument	Geomax Zenith15, 06GPS
	GCP geolocation accuracy	1-2cm
	GCP and photo merging	Pix4D
	Coordinate system	Amersfoort/RD New (EGM 96 Geoid), EPSG: 28992
Radiometric correction	Downwelling Light Sensor used	yes
	Calibration reflectance panel	yes
	Processing and calibration	Pix4D
	Setting	Camera, Sun Irradiance and Sun Angle using DLS IMU

Appendix 2, data processing parameters

Optical survey

PG: Import/reference	Software	Pix4D Mapper 4.5.7
	Batch/Chunks	1
	Geolocated images	399
	Quality check	Manual
	CRS camera	WGS84 (EGM 96 Geoid), EPSG: 4326
	CRS GCPs	Amersfoort/RD New (EGM 96 Geoid), EPSG: 28992
	CRS output	Amersfoort/RD New (EGM 96 Geoid), EPSG: 28992
	Camera model	FC6520_DJIMFT115mmF1.7AS-PH_15.0_5280x3956
	Geolocation accuracy	Horz: 5m Vert: 10m
	Manual corrections	Set altitude to 45m
	Mean Reprojection Error	0.220 pixels
	GCPs used	8
	GCP accuracy	mean RMS error = 0.051m
PG: Alignment/sparse PC	Keypoint Image Scale	Full
	Calibrated/aligned images	399
	Matching type	Aerial Grid or Corridor
	Matching settings	None
	Key point extraction	Automatic (10.000 per image)
	Tie point extraction	N/A
	Calibration method	Standard

	Int. parameters optim.	All
	Ext. parameters optim.	All
	Rematch	Auto
	Other settings	N/A
PG: Dense PC	Image scale/quality	Multiscale, ½ (half image size, default)
	Point density	Optimal
	Minimum # of matches	3
	Number of points	44.453.227
	Classification	Yes (Pix4D method)
	Other settings	N/A
PG: 3D model	Source data	PC
	Surface type	N/A
	Octree depth	High (14)
	Face count	High (max. 5.000.000)
	Texture size	High (16384x16384)
	Texture source data	N/A
	Texture type	N/A
	Mapping mode	N/A
	Blending mode	N/A
	Colour balancing	No
	Other settings	N/A
PG: ortho	GSD	1.01cm/pixel
	Source data	N/A
	Blending mode	N/A
	Other settings	N/A
PG: DSM	GSD	1.01cm/pixel
	Source data	N/A
	Noise filter	Yes
	Surface smoothing	Yes
	Type	Sharp
	Method	IDW
PG: DTM	GSD	1.01cm/pixel
	Point classes	N/A
PG: index	GSD	N/A
	Radiom. correction type	N/A
	Calibration	N/A
	Reflectance map	N/A
	Index and calculation	N/A
Enhanced visualisation	Software	QGIS 3.28.0
	Visualisation	Multiband colour
	Colour ramp	N/A
	Processing	None

	Filter	None
	Settings	None

Multispectral survey

PG: Import/reference	Software	Pix4D Mapper 4.5.7
	Batch/Chunks	5 (R/G/B/RE/NIR)
	Geolocated images	2690
	Quality check	Manual
	CRS camera	WGS84 (EGM 96 Geoid), EPSG: 4326
	CRS GCPs	Amersfoort/RD New (EGM 96 Geoid), EPSG: 28992
	CRS output	Amersfoort/RD New (EGM 96 Geoid), EPSG: 28992
	Camera model	RedEdge-M_5.5_1_1280x960 (R/G/B/RE/NIR)
	Geolocation accuracy	Horz: 5m Vert: 10m
	Manual corrections	Set altitude to 45m
	Mean Reprojection Error	0.160 pixels
	GCPs used	8
	GCP accuracy	mean RMS error = 0.384m
PG: Alignment/sparse PC	Keypoint Image Scale	Full
	Calibrated/aligned images	2690
	Matching type	Aerial Grid or Corridor
	Matching settings	None
	Key point extraction	Automatic (10.000 per image)
	Tie point extraction	N/A
	Calibration method	Alternative
	Int. parameters optim.	All
	Ext. parameters optim.	All
	Rematch	Auto
	Other settings	N/A
PG: Dense PC	Image scale/quality	Multiscale, ½ (half image size, default)
	Point density	Low
	Minimum # of matches	3
	Number of points	893.554
	Classification	No
	Other settings	N/A
PG: 3D model	Source data	N/A
	Surface type	N/A
	Octree depth	N/A
	Face count	N/A

	Texture size	N/A
	Texture source data	N/A
	Texture type	N/A
	Mapping mode	N/A
	Blending mode	N/A
	Colour balancing	N/A
	Other settings	N/A
PG: ortho	GSD	N/A
	Source data	N/A
	Blending mode	N/A
	Other settings	N/A
PG: DSM	GSD	N/A
	Source data	N/A
	Noise filter	N/A
	Surface smoothing	N/A
	Type	N/A
	Method	N/A
PG: DTM	GSD	N/A
	Point classes	N/A
PG: index	GSD	3.25cm/pixel
	Radiom. correction type	Camera and Sun Irradiance using DLS IMU
	Calibration	Yes (with reflectance target)
	Reflectance map	Yes
	Index and calculation	R, G, B, RE, NIR NDVI = (NIR-R)/(NIR+R)
Enhanced vis.: DSM	Software	QGIS 3.28.0
	Visualisation	Singleband pseudocolour
	Colour ramp	Various
	Processing	None
	Filter	DSM – local cumulative cut stretch (set by window extents, default settings)
	Settings	None

Appendix 3, schema of documented metadata for anomaly mapping and interpretation

Item	Description	Values	Comments
Id	Anomaly number	1-x	Simple enumerator
Rec_moment	Recording moment	E.g., 'winter', 'February, or a more specific date	Used to organize GIS layers
Sensor_vi	Sensor Visualisation	E.g., 'opt_ortho' (optical sensor, orthophoto visualization) or 'multi_ndvi' (multispectral sensor, NDVI visualization)	The sensor and the specific data model used for the mapping of anomalies; refers to 4.1.2 Data processing and derivation of products
Source_lay	Source Layer	E.g., 'dem_1cmres' (LiDAR DEM data with a 1cm resolution) or 'autumn_120m_corrected_with_LP_30m' (Thermal mosaic recorded at 120m with a Low Pass filter using a 30m radius)	The specific visualization of the data used for the mapping of anomalies; refers back to 4.1.2 Data processing and derivation of products
Anoma_int	Interpretation of anomaly source	E.g., 'ditch outline', 'rectangular elevation', 'subsoil stone feature'	Initial mapping of all features that are not explained or not directly explained by natural or modern anthropomorphic activity
An_confid	Confidence of anomaly interpretation	0-3	'0' none (anomaly type is unknown), '1' low (anomaly interpretation is questionable), '2' medium (anomaly is clearly visible and there are analogies to the confirmed interpretation in the area, but the morphology is not distinct), '3' high (anomaly clearly visible and has a distinct form (adapted from Lozić and Štular 2021)
Visibility	How well is the anomaly visible	1-2	Referring to the local contrast that led to identification of the anomaly; '1' is poor and '2' is good (adapted from Lozić and Štular 2021)

Veget_dens	How dense is the vegetation locally	1-3	Referring to local vegetation density that may obscure full identification of the anomaly; '1' negligible, '2' medium (introduces occasional and/or moderate noise) or '3' high (introduces constant and/or significant noise) (adapted from Lozić and Štular 2021)
Author	Author	E.g., 'JW' (Jitte Waagen)	The person that performs the anomaly and interpretative mapping
Date	Date	E.g., '12-04-2023'	Date of the anomaly and interpretative mapping
Arch_int	Archaeological interpretation of anomaly	E.g., 'moat outline', 'structure boundary', 'stone debris of collapsed wall'	Interpretation of anomaly in terms of the most probable archaeological explanation
Arch_confi	Confidence of archaeology interpretation	0-3	'0' none (interpretation is very uncertain), '1' low (interpretation is questionable), '2' medium (interpretation is plausible and there are analogies to the confirmed interpretation in the area, but the morphology is not distinct), '3' high (interpretation is quite certain and has a distinct form (adapted from Lozić and Štular 2021)